

1 Reliable inference of phylogenomic relationship via assembly-based strategy 2 accommodating raw reads and proteins

3 Yunlong Li^{1,2#*}, Xu Liu^{1,2#}, Chong Chen³, Jian-Wen Qiu⁴, Kevin Kocot⁵, Jin Sun^{1,2*}

4
5 ¹ Key Laboratory of Evolution & Marine Biodiversity (Ministry of Education) and Institute of
6 Evolution & Marine Biodiversity, Ocean University of China, Qingdao 266003, China

7 ² Laboratory for Marine Biology and Biotechnology, Qingdao Marine Science and Technology
8 Center, Laoshan Laboratory, Qingdao 266237, China

9 ³ X-STAR, Japan Agency for Marine-Earth Science and Technology (JAMSTEC), 2-15
10 Natsushima-cho, Yokosuka, Kanagawa 237-0061, Japan

11 ⁴ Department of Biology, Hong Kong Baptist University, Hong Kong, China

12 ⁵ Department of Biological Sciences and Alabama Museum of Natural History, University of
13 Alabama, Tuscaloosa, AL 35487, USA

14
15 # Equal contribution

16 * Corresponding author: Jin Sun, jin_sun@ouc.edu.cn; Yunlong Li, ylyfy@connect.ust.hk

18 **Abstract**

19 Phylogenomics has emerged as a transformative approach in systematics, conservation biology,
20 and biomedicine, enabling the inference of evolutionary relationships by leveraging hundreds
21 to thousands of genes from genomic or transcriptomic data. However, acquiring high-quality
22 genomes and transcriptomes necessitates samples with intact DNA and RNA, substantial
23 sequencing investments, and extensive bioinformatic processing, such as
24 genome/transcriptome assembly and annotation. This challenge is particularly pronounced for
25 rare or difficult-to-collect species, such as those inhabiting the deep sea, where only fragmented
26 DNA reads are often available due to environmental degradation or suboptimal preservation
27 conditions. To address these limitations, we introduce VEHoP (Versatile, Easy-to-use
28 Homology-based Phylogenomic pipeline), a tool designed to infer protein-coding regions from
29 diverse inputs, including raw reads (short and long), draft genomes, transcriptomes, and
30 annotated genomes. VEHoP automates the generation of orthologous sequence alignments,
31 concatenated matrices, and phylogenetic trees, streamlining phylogenomic analyses for
32 researchers across disciplines. The tool aims to (1) expand taxonomic sampling by
33 accommodating a wide range of input data types and (2) simplify phylogenomic workflows,
34 making them accessible to researchers with varying levels of bioinformatic expertise. We
35 evaluated VEHoP's performance using datasets from oysters, catfish, and insects,
36 demonstrating its ability to produce robust phylogenetic trees with strong bootstrap support,
37 outperforming assembly-free methods. Additionally, we applied VEHoP to reconstruct the
38 phylogeny of the enigmatic deep-sea gastropod order Neomphalida, successfully resolving a

39 well-supported phylogenetic backbone for this poorly understood group. VEHoP is freely
40 available on GitHub (<https://github.com/ylify/VEHoP>), with dependencies easily installable
41 via Bioconda.

42

43 **Keywords:** phylogenomics, reads, phylogeny, evolution, pipeline, deep sea

44

45 **Background**

46 Phylogenetics is now the most fundamental method in evolutionary biology research to
47 understand and illuminate the relationships between organisms. Multiple types of data can be
48 used to infer phylogenetic relationships, including phenotypic and genotypic characteristics.
49 Among them, biological molecules (i.e., nucleic acids and amino acids) are widely used for
50 reconstructing phylogenetic trees. At the early stages of molecular phylogeny, one or a few
51 gene markers were used, such as the mitochondrial cytochrome *c* oxidase subunit I (COI),
52 NADH dehydrogenase subunit 4 (NAD4), nuclear ribosomal RNA genes, or the combination
53 of them (Hao et al. 2015; Ibáñez et al. 2019). With the improvement of sequencing techniques,
54 this was followed by mitogenome-based reconstructions (Donath et al. 2019; Irisarri et al. 2020;
55 Ghiselli et al. 2021). However, these gene trees sometimes failed to reveal the true relationships
56 among taxa due to introgression, different gene evolutionary rates between groups, and long-
57 branch attraction (Doolittle and Logsdon Jr 1998; Huynen and Bork 1998; Doolittle 1999;
58 Degnan and Rosenberg 2006). This called for more sophisticated methods for phylogenetics
59 that can address all such issues. Recently, with the development of next-generation sequencers,
60 phylogenetics based on genome-level data (i.e., phylogenomics) has become a focus in many
61 fields (Dunn et al. 2008; Young and Gillung 2020).

62

63 It has been shown that taxon sampling is key in reducing errors in phylogenetic inferences
64 (Powell and Battistuzzi 2022). Despite this, in most cases, it is unrealistic to gather sufficient
65 data on all target species to answer the phylogenetic questions. For one, some species inhabit
66 inaccessible environments, such as the deep sea and polar regions, or maybe extremely rare
67 that only one or few specimens are available as long-preserved samples in natural history
68 museums. Also, species distribution in certain groups can be skewed, which leads to biased
69 sampling. In these cases, researchers would have to perform a phylogenetic reconstruction
70 using a dataset lacking some species. If those species happen to represent an important node,
71 the tree topology may be changed based on such an imbalanced taxon-sampling dataset. In
72 addition, most extinct fossil species cannot be sequenced, thus rendering it impossible for
73 molecular phylogenies to include all taxa on the tree of life across evolutionary history
74 (Marshall 2017).

75

76 There is no doubt that genome-based phylogeny contains much more information than single
77 or few gene makers (Chang et al. 2011). As next-generation sequencing (NGS) technology
78 advanced, more and more sequenced genomes and transcriptomes have been released to the
79 public at an elevated rate year after year (Turnbull et al. 2023). Nevertheless, many of these
80 datasets were sequenced initially for organelle genome assembly, genome survey, genome
81 annotation, gene expression level analysis, and so on. These are all potential sources for
82 phylogenetics, yet they often remain buried deep in the public database.

83

84 The best datasets for phylogenomic analysis are whole genome data from different species
85 (Cheon et al. 2020; Fleming et al. 2023). Yet, the situation is often complicated in practical use.
86 In many groups, only a few well-annotated genomes are available while the rest are
87 transcriptomes and raw Illumina DNA reads. To obtain a genome dataset for phylogenomic
88 analyses from these, multiple steps of bioinformatics analyses must be performed (Liu et al.
89 2023), which always include quality control of the raw data, draft genome assembly and
90 annotation (Simão et al. 2015). Apart from these, ortholog inference must be performed to
91 identify sequences whose evolutionary history reflects that of the species, which may be the
92 most important step for reliable phylogenomic reconstructions (Yang and Smith 2014;
93 Mongiardino Koch 2021; Lozano-Fernandez 2022). Finally, matrix assembly must be
94 performed, which involves further steps such as alignment, trimming of ambiguously aligned
95 positions, concatenation, and tree reconstruction. The whole workflow is time-consuming and
96 can be confusing for those researchers not from a bioinformatics background (Dylus et al.
97 2023).

98

99 Some tools for phylogenomic analysis can use raw sequencing reads to generate phylogenetic
100 trees, such as Read2Tree (Dylus et al. 2023). However, the reference OMA (“Orthologous
101 MAtrix”) database designated in Read2Tree is not fully customized, and the current procedure
102 for the phylogenetic reconstruction is sophisticated with many manual curation steps. MIKE
103 (Wang et al. 2024) is a MinHash-based and *k*-mer phylogenetic algorithm developed for large-
104 scale next-generation sequencing data. GeneMiner (Xie et al. 2024) is a toolkit developed for
105 phylogenetic marker mining, which extracts markers from transcriptomic, genomic, or other
106 next-generation sequencing (NGS) or third-generation sequencing (TGS) data. It could be
107 used for multiple gene phylogeny, yet it is still inefficient in phylogenomic analysis due to
108 vague instructions and low numbers of single-copy orthologs extracted.

109

110 To address these problems, we here developed a new pipeline which we name ‘VEHoP’
111 (Versatile, Easy-to-use Homology-based Phylogenomic pipeline). The VEHoP workflow
112 allows different types of datasets as input, including raw reads, genomic DNA assemblies,
113 transcriptomes, well-annotated genomes, or any combinations thereof. After providing these
114 files as the input, users only need to provide a prefix for the run, a path to the database (required
115 if DNA assemblies or transcriptomes are provided), and the optional adjustment of quality
116 control in matrix assembly (e.g., occupancy and alignment threshold, 2/3 and 100 AAs by
117 default, respectively). Alternative analyses can be specified if needed, such as PhyloBayes,
118 ASTRAL, set up occupancy. The output files include single-gene alignments, single-gene trees,
119 a concatenated supermatrix, and results of phylogenetic analyses using the supertree and
120 supermatrix-based approaches.

121

122 To assess and benchmark the performance of the VEHoP, we tested it in three benchmarking
123 groups with well-annotated references. Ostreida (the ‘oyster’ order) is a well-studied group of
124 animals in phylum Mollusca with 10 high-quality and well-annotated genomes plus a range of
125 transcriptome datasets, making it an ideal clade for benchmarking the performance and
126 reliability of VEHoP. The other two groups of fish and insects were also selected to verify the
127 feasibility of VEHoP. To further test the applicability of VEHoP in resolving phylogenetic
128 issues, we also used it to analyze a dataset of the gastropod order Neomphalida which is a deep-
129 sea clade of typically small-sized animals. Previously phylogenetic analyses did not fully
130 resolve the internal relationships within this order, due to the lack of high-quality genomes and
131 transcriptomes required by traditional phylogenomic pipelines, and thus the evolutionary
132 relationships among the neomphalidan taxa remained highly contentious. Our results lend
133 support to the VEHoP as a user-friendly, efficient, and accurate workflow.

134

135 **Description of VEHoP**

136 Input files and parameters

137 The VEHoP pipeline accepts raw reads, draft genome, transcriptome sequencing data, and well-
138 annotated genomes, or any combination of these data types. Raw reads can be NGS or TGS,
139 which could be configured in input with the tab-delimited text (prefix in output; supporting
140 type: NGS, HiFi, ONT, or RNA; read path; read path). It also allows the SRA accession number
141 instead of the local path, which is compiled to download data from NCBI automatically. The
142 raw data will go through a simple, coarse assembly using a *de novo* assembler, such as
143 MEGAHIT (Li et al. 2015) for genomic data (i.e., NGS), Trinity (Haas et al. 2013) for
144 transcriptome data (i.e., RNA), hifiasm (Cheng et al., 2021) for HiFi and Shasta (Shafin et al.,
145 2020) for nanopore reads (i.e., ONT), after quality control and trimming procedures. Other
146 inputs should be in *fasta* format, but with different suffixes: *.pep.fasta* for proteomes from
147 quality datasets, *.transcript.fasta* for transcriptomes, and *.genomic.fasta* for DNA genomic
148 assemblies. All these assembling procedures can be customized in a VEHoP *.config* file, instead
149 of sophisticated manual operations one by one. In addition, the user also needs to prepare a
150 database for homolog extraction, if genomic or transcriptomic reads or assemblies are provided.
151 The reference database could be a concatenation of protein files suggested from close relatives
152 with well-annotated genomes. By default, VEHoP uses 40 threads (-t 40) throughout, including
153 *de novo* assembly, homolog-inference using miniprot, OrthoFinder processing, matrix
154 assembly and tree construction. During the matrix assembly, VEHoP keeps the quality single-
155 gene alignments with the threshold of alignment length (-l 100) and taxonomy occupancy (2/3,
156 users could adjust manually via setting the minimum samples, -m #s).

157

158 Workflow

159 The pipeline was coded in Python. All dependencies can be easily installed via Anaconda (Fig.
160 1) and implemented as follows, except HmmCleaner (Di Franco et al. 2019) which the user
161 can install optionally by the instructions provided in the GitHub repository.

162 The workflow consists of the following steps (Fig. 1), which can be implemented using a single
163 command:

164 1) Draft assembly from reads based on the content of a configured text, with SRA download
165 (if applicable) and *de novo* assembly, including Trinity for RNA-seq (NGS in paired-end or
166 single-end mode), Megahit for metagenome from NGS, hifiasm for HiFi reads, and Shasta for
167 nanopore reads; 2) miniprot (Li 2023) is used to map protein sequences from the reference
168 database to the coarsely assembled genomic or transcriptomic data to predict gene models; 3)
169 TransDecoder (Douglas 2018) and embedded Python are used to extract quality proteins based
170 on the predicted gene models (no stop codon in the sequences except for the last one and length
171 above threshold); 4) cd-hit (Fu et al. 2012) is performed to remove redundant sequences with
172 the threshold of 85% similarity; 5) the filtered protein sequences are submitted to OrthoFinder
173 (Emms and Kelly 2019) to identify orthogroups (OGs), with the occupancy assigned by the
174 user (default 2/3, and only orthologs matching the standard will be kept); 6) redundant
175 sequences are removed with uniqHaplo while the remaining sequences are aligned with
176 MAFFT (Katoh and Standley 2013) with default settings; 7) the misaligned regions are
177 removed with HmmCleaner and the aligned files are trimmed with BMGE (Crisuolo and
178 Gribaldo 2010) and trimAL (Capella-Gutiérrez et al. 2009); 8) AlignmentCompare
179 (https://github.com/DamienWaits/Alignment_Compare) is then used to remove sequences
180 shorter than 20 amino acids (AAs), followed by a second occupancy check to make sure all
181 sequences overlap, which is necessary for single-gene tree reconstructions; 9) IQ-TREE or
182 FastTree (default being FastTree) is used to build trees for each filtered OGs. 10)
183 PhyloPyPruner is used to remove paralogs in the filtered alignments; 11) The generated
184 supermatrix is used to reconstruct phylogenetic trees, using IQ-TREE (Minh et al. 2020),
185 FastTree (Price et al. 2010), and PhyloBayes (Lartillot et al. 2013); 12) A random subsample
186 of the initial matrix to 2,500,000 and 5,000,000 sites can also be performed for the reconstruction
187 of phylogenetic relationships using IQ-TREE and PhyloBayes. Apart from concatenation-
188 based phylogeny, the pipeline provides a coalescent phylogenetic approach (default: off)
189 implemented via ASTRAL (Mirarab et al. 2014).

190

191 Output files

192 The output files of the workflow include an initial data matrix in .fasta format, an IQ-TREE
193 tree file, and a FastTree tree file. Apart from the above-mentioned default outputs, the results
194 of ASTRAL and PhyloBayes can also be found in the final output directory if related settings
195 are specified in the commands. If users want to attempt more phylogenetic analyses, they can
196 perform additional custom analyses using the initial data matrix.

197

198 **Results**

199 *Benchmark test 1: Oyster dataset*

200 To benchmark the usability and efficiency of the workflow, we collected data from
201 representatives of Ostreida as an example. The datasets include 10 species from Ostreida
202 including *Pinctada fucata*, *Crassostrea hongkongensis*, *C. angulata*, *C. ariakensis*, *C. nippona*,
203 *Ostrea edulis*, *O. denselamellosa*, *C. virginica*, *C. gigas*, *Saccostrea glomerata*, and two species
204 from the closely related order Pectinida (as the outgroup), *Pecten maximus* and *Mizuhopecten*
205 *yessoensis*. The data included well-annotated genomes, draft genomes from NGS reads, and *de*
206 *novo* transcriptomes from RNA-seq. The sources of these data are included in the
207 Supplementary Table S1.

208

209 We tested our workflow with different datasets, including the following. Dataset 1: well-
210 annotated genomes, whose output was labelled as “reference topology” in Fig. 2; dataset 2:
211 NGS raw reads; dataset 3: transcriptome reads, assembled with Trinity; and dataset 4: a dataset
212 combination including all three types of abovementioned data. For each dataset, the occupancy
213 was set to 2/3, and phylogenetic analyses were performed with two efficient algorithms IQ-
214 TREE (MFP) and FastTree, based on maximum likelihood estimation. The analyses resulted
215 in the same branching order between the reference topology from well-annotated genomes and
216 that from NGS raw reads (Fig. 2a). All bootstrap values reached 100 in these two trees, except
217 for two nodes in NGS reads dataset, with a bootstrap value of 68 within the genus *Crassostrea*.
218 However, the position of *C. nippona* was different from reference topology when using dataset
219 3 (transcriptomes), though the bootstrap of all nodes reached 100 (Fig. 2a). Furthermore, the
220 same phylogenetic methods were performed on the matrix of 2973 orthologs generated from
221 genome-wide proteins, genome sequences, and transcriptomes, which showed that most of the
222 terminals were clustered by species, except that *C. gigas* was mixed with its most closely
223 related species *C. angulata* (Supplementary Fig. 1).

224

225 To better understand how much data is sufficient to reconstruct reliable phylogenetic
226 relationships, we subsampled the *C. hongkongensis* data into 2X, 4X, 6X, and 8X of its genome
227 size. Based on these datasets, we performed phylogenetic analyses using IQ-TREE (MFP) and
228 FastTree. The results showed that the pipeline worked well with all the datasets: the branching
229 order of the trees was identical to reference topology, and all node supports were 100%
230 (Supplementary Fig.2). Reduced datasets for every species (1 Gb, 2 Gb, 4 Gb, 6 Gb, and 8 Gb)
231 were also made and phylogenetic analyses conducted (see Supplementary Table S2 for details).
232 The results showed that branch order became unstable for the 1 Gb and 2 Gb datasets, resulting
233 in paraphyly within *Crassostrea*. For datasets larger than 2 Gb, the VEHoP was able to recover
234 phylogenetic relationships from well-annotated genomes, at least at the genus level

235 (Supplementary Fig. 1). The total run time was also recorded for these different datasets to test
236 the performance. For the reduced datasets, it took 4.24, 10.22, 18.60, 25.46, and 27.32 hours
237 to obtain the two tree files, one generated by FastTree and another one generated by IQ-TREE,
238 respectively. As for the full-size mixed dataset, it took VEHoP 54.38 hours to obtain the results,
239 showing the clusters from same species (except the NGS data from *C. angulata*) and the
240 consistent branching order with reference (Supplementary Table S3).

241
242 Read2Tree (Dylus et al. 2023) was also performed on the reduced datasets and full-size
243 genomic datasets. Marker genes of the only three mollusc species available on the OMA
244 database, including the oyster *C. gigas*, the octopus *Octopus bimaculoides*, and the true limpet
245 *Lottia gigantea*, were downloaded from the OMA Orthology database as mapping references.
246 For the 1G dataset, Read2Tree took 7.79 hours to get a *.nwk* format tree file, with *Pecten*
247 *maximus* incorrectly grouped with two reference species from the OMA database
248 (Supplementary Fig. 3). As for the 2G dataset, 19.56 hours were used to generate the tree, yet
249 the position of *C. nippona* was inconsistent with the genome-based tree, though the bootstrap
250 of this node was 100%. In the 4G dataset, a total of 18.5 hours was used, resulting in the same
251 branching order as that in the 2G dataset. For 6G, 8G, and full-size datasets, 21.75, 27.55, and
252 43.83 hours were used for each dataset, respectively, and they all shared the same branching
253 order as that of the 2G dataset. The total run time for each dataset can also be found in
254 Supplementary Table S3.

255
256 MIKE was also performed to benchmark the performance of the VEHoP pipeline with different
257 sizes of datasets, in addition to Read2Tree. In 1G, 2G, 4G, 8G, and full-size datasets,
258 *Saccostrea glomerata* nested with *Crassostrea* or within *C. virginica*, causing paraphyly. Only
259 in the 6G dataset, the topology was well-resolved and consistent with the current understanding
260 of oyster phylogeny at the genus level (Li et al. 2021) (Supplementary Fig. 4). The run time of
261 MIKE for different sizes of datasets can be found in Supplementary Table S4.

262
263 The root-to-tip distances for each species were calculated using various tree files to assess tree
264 quality. The distances of each tip in reference topology (well-annotated genomes) were
265 employed to normalize the corresponding distances in other trees (Supplementary Table S5).
266 The findings showed the similar root-to-tip distances to reference topology, whereas the trees
267 produced by Read2Tree displayed significant variance compared to the other results (Fig. 2b).
268 The root-to-tip distances in MIKE is not applicable for quantification.

269
270 *Benchmark test 2: Catfish dataset*

271 The fish datasets include 9 catfishes from the order Siluriformes: *Bagarius yarrelli*, *Clarias*
272 *gariepinus*, *Hemibagrus wyckioides*, *Ictalurus punctatus*, *Pangasianodon hypophthalmus*,

273 *Silurus asotus*, *Silurus meridionalis*, *Tachysurus fulvidraco* and *Trichomycterus rosablanca*.

274 The common carp *Cyprinus carpio* and the zebrafish *Danio rerio* were used as outgroups. The
275 datasets include well-annotated genomes, NGS raw reads and public draft assemblies from
276 NCBI. The source of these data can be found at Supplementary Table S1.

277
278 Three datasets were used in this benchmark test, including dataset 1: well-annotated genomes
279 dataset 2: NGS raw reads. VEHoP, Read2Tree and MIKE were applied on dataset 2, whose
280 topologies can be found in Fig. 2c. Other than that, an additional IQ-TREE (MFP) procedure
281 was also performed on the matrix generated by Read2Tree. IQ-TREE (MFP) and IQ-TREE
282 (C60) were performed based on the matrix generated by VEHoP in both two datasets. And for
283 comparing, the topology generated by IQ-TREE (MFP) based on well-annotated genomes, in
284 this case, dataset 1, was chosen to be the reference topology. VEHoP showed a great
285 consistence and stability in NGS reads (dataset 2), while Read2Tree and MIKE both resulted
286 in rather different topologies compared to the reference topology (Fig. 2c). The topology
287 generated by Read2Tree showed that *H. wychioides* grouped together with the outgroup species,
288 and *Sasotus* came to the basal position of the ingroup instead of *T. rosablanca*. The genus
289 *Silurus* was recovered as paraphyletic. In MIKE, the outgroup species *C. carpio* nested within
290 catfishes. And the genus *Silurus* became basal instead of *T. rosablanca*. *C. gariepinus* nested
291 deep inside of the ingroup catfish species, while in the reference topology, it was positioned at
292 the location of the secondary basal node. Root-to-tip distance was also calculated and
293 normalized for each tree file generated (Supplementary Table S5); all results generated by
294 VEHoP demonstrated a high level of consistency (Fig. 2d). All original tree topologies can be
295 found in Supplementary Fig. 5.

296

297 *Benchmark test 3: Insect dataset*

298 The insect datasets include 8 species from the superorder Condylgnatha, which comprises of
299 two orders: Thysanoptera (thrips) and Hemiptera (true bugs). These species are *Acyrtosiphon*
300 *pisum*, *Aphis gossypiii*, *Bemisia tabaci*, *Frankliniella occidentalis*, *Nilaparvata lugens*,
301 *Planococcus citri*, *Ranatra chinensis* and *Thrips palmi*. And two species from Psocodea were
302 selected as outgroups: *Pediculus humanus corporis* and *Menopon gallinae*. The datasets used
303 in this study also include well-annotated genomes, NGS raw reads and public genome
304 assemblies from NCBI, whose data source can also be found at Supplementary Table S1.

305

306 The dataset composition in this benchmark test was the same as that in benchmark test 2:
307 including dataset 1: well-annotated genomes; dataset 2: NGS raw reads. The methodology used
308 was the same as for the catfish case study. The results generated by VEHoP shared the same
309 branch order as the reference topology (i.e., inferred from well-annotated genomes), who
310 successfully recovered the monophyletic relationship of Thysanoptera and Hemiptera. But in

311 Read2Tree and MIKE, they both resulted in inconsistent branch orders compared to reference
312 topology (Fig. 2e) In Read2Tree, Hemiptera was successfully recovered as monophyletic, yet
313 *N. lugens* was assigned to Thysanoptera incorrectly. And in MIKE, *M. gallinae* nested within
314 Hemiptera as an outgroup species. Besides, both Hemiptera and Thysanoptera were not
315 analyzed as monophyletic groups. The inconsistency can also be found in the root-to-tip
316 distance results in Fig. 2f. All original tree topologies can be found in Supplementary Fig. 5.

317

318 *Case study: Neomphalidan snails*

319 The molecular phylogeny of deep-sea endemic neomphalidan gastropods has long been
320 contentious, partially due to insufficient sampling, small body size and tissue quantity, and
321 lacking many sequences. Here, we applied VEHoP on the original Illumina sequencing dataset
322 (see Supplementary Table S6 for details) used to assemble the mitochondrial genomes from a
323 previous study (see Zhang et al., 2024), which generated a matrix consisting of 1899 orthologs
324 with an occupancy of 2/3. In addition, to improve taxon sampling, we newly sequenced a
325 specimen of *Neomphalus fretterae* (collected from Tempus Fugit vent field, Galápagos Rift,
326 0°46.1954'N / 85°54.6869'W, 2561 m deep, R/V *Falkor (too)* cruise FKt231024, remotely
327 operated vehicle (ROV) *SuBastian* dive #609, 2023/Nov/02) following the same methods as
328 Zhang et al. (2024). Four species of Cocculinida (*Cocculina enigmadonta*, *C. tenuitesta*, *C.*
329 *japonica*, *C. subcompressa*), the sister-order of Neomphalida were used as outgroups, as well
330 as the more distantly related vetigastropod snails *Tristichotrochus unicus* and *Steromphala*
331 *cineraria*. The data of *C. enigmadonta*, *C. tenuitesta*, *Lamellomphalus manusensis*, *Lirapex*
332 *politus*, *Symmetriapelta wreni*, *Melanodrymia laurelin*, *Melanodrymia telperion*,
333 Neomphalidae gen et sp. *Hatoma sensu* Zhong et al., 2022, *Nodopelta heminoda*, and
334 *Symmetriapelta becki* were gathered from previous studies, which were used to assemble
335 mitochondrial genomes for phylogeny (Zhong et al. 2022; Zhang et al. 2024).

336

337 We first attempted to reconstruct the molecular phylogeny of Neomphalida using mitochondrial
338 genomes with multiple models in IQ-TREE, including MFP, C20, C40, and C60 based on the
339 matrices from Zhang et al. (2024). This revealed two distinct tree branching orders with nearly
340 equal support from different sequencing matrices (see Supplementary Fig. 6, confirming the
341 same situation encountered also in a previous study (Zhang et al., 2024). We then conducted
342 multiple phylogenetic analyses through VEHoP based on the assemblies of the
343 abovementioned datasets, including IQ-TREE with the MFP model, Site-specific frequency
344 models (including C20, C40, and C60), and FastTree. All these analyses resulted in the same
345 tree branching order with maximum support in each node, except for one node in Peltospiridae
346 which had the bootstrap value of 85 in the C20 model (Fig. 3). Apart from VEHoP, Read2Tree
347 and MIKE were also performed on the same dataset of Neomphalida. However, these two
348 methods were unable to resolve a consistent topology, even at the order level (Supplementary
349 Fig. 7).

350

351 **Discussion**

352 We present VEHoP, a new pipeline for phylogenomic analyses with the flexibility of using
353 publically genomic assemblies, well-annotated genomes, NGS raw reads, RNA-seq raw reads,
354 or a combination of these data. This workflow allows users to reconstruct phylogenetic trees
355 with one single command, significantly lowering the technical hurdle for researchers to carry
356 out phylogenomic inferences. VEHoP is able to reconstruct congruent and robust relationships
357 among taxa using fragmented draft genomes that were rapidly assembled from NGS reads,
358 with results comparable with trees generated from well-annotated genome datasets.

359
360 Currently, most available phylogenomic pipelines are based on protein datasets (Kocot et al.
361 2011; Sun et al. 2021), which require cumbersome steps and are time-consuming to prepare.
362 To obtain high-quality protein files, high-quality DNA sequencing data is inevitably needed.
363 Furthermore, it is necessary to conduct genome assembly to get a contig- or scaffold-level draft
364 genome, followed by gene model prediction. This workflow usually takes several days just for
365 one single species even with ample computing resources.

366
367 There is a vast amount of data in public databases, including unannotated genomes and raw
368 NGS reads (genome skimming projects previously used in organelle assemblies or genome
369 surveys), which have been underutilized in phylogenomic studies. Understandably, these data
370 vary in quality and coverage, and thus it has been challenging to use them for phylogenetic
371 analysis. With VEHoP, however, researchers can extract homologs from these genomic data at
372 ease, with the potential to greatly enhance taxon sampling and produce a more robust and
373 consistent tree topology in phylogenetic analyses. As an example, we generated pie charts for
374 major lophotrochozoan animal phyla to show the potential of these ‘buried’ data in
375 phylogenetics based on NCBI data (Fig. 4 and Supplementary Table S7, data up to May 2024).
376 Among Mollusca, for example, there are only 286 species with genome assemblies (only a
377 small fraction of these is annotated) while an additional 896 species have transcriptomic data.
378 These two data types are mostly commonly used source data for phylogenomic analysis. With
379 VEHoP, we can further include 325 species which lack both genome and transcriptome data
380 but with DNA genomic data, greatly expanding the taxon coverage.

381
382 In our benchmarking study using various data types from oysters (benchmark test 1), VEHoP
383 showed a high speed and accuracy in inferring phylogeny. The branching order inferred based
384 on unannotated genomic data was the same as that based on well-annotated genomes, though
385 not all node support reached 100%. For the RNA data, we attempted two strategies: 1)
386 extracting homologs directly from assembled transcripts with miniprot; 2) predicting proteins
387 with TransDecoder. Those two strategies resulted in the same branching order, and each node
388 reached 100% support. However, the branching order from this analysis differed from those

389 based on well-annotated genomes. This discrepancy was probably due to the presence of
390 isoforms in the transcriptomes, which made it difficult to distinguish homologs from paralogs,
391 leading to the different branching orders in the transcriptome-based trees (Cheon et al. 2020).
392 Thus, genomic data is still recommended when available. Nonetheless, the miniprot-based
393 strategy in transcripts could be a more accurate way compared with TransDecoder strategy in
394 tree construction and still highly robust at the genus level, since the transcripts were obtained
395 by blasting with closely relatives, which in some cases, would reduce the impact of
396 contamination.

397
398 We also tested Read2Tree (Dylus et al. 2023) with the same datasets and made a comparison
399 with VEHoP. Read2Tree only accepts marker genes from the OMA database, where only three
400 mollusc species are currently available. We used marker genes of these abovementioned
401 species as a reference to reconstruct phylogenetic trees with Read2Tree. Both Read2Tree and
402 VEHoP were not able to reveal the same branching order as that of the high-quality genome
403 dataset. The position of *Crassostrea nippona* was unstable. However, VEHoP successfully
404 recovered the same branching order as the same as reference topology inferred from well-
405 annotated genomes, while Read2Tree retained the branching order with low-coverage datasets.
406 As for run time comparison, VEHoP performed much quicker with dataset less than 4G. After
407 4G, Read2Tree took less time than VEHoP, since it reconstructed trees directly from raw
408 sequencing reads, and VEHoP needed to assemble the reads first before proceeding with
409 phylogenetic reconstruction. Apart from Read2Tree, MIKE was also tested with the same
410 datasets mentioned above. Though the total run time of MIKE was much less than both
411 Read2Tree and VEHoP, the branching orders generated by MIKE were unstable in most
412 datasets. *Saccostrea glomerata* grouped within *Crassostrea* in most cases (Supplementary Fig.
413 3), with the sole exception of the 6G dataset, where *S. glomerata* grouped with *Ostrea*. Besides,
414 none of the branch order were the same as reference topology ([Supplementary Fig. 4](#)).
415 Compared with Read2Tree and MIKE, VEHoP accepts all three types of input data, including
416 proteins from well-annotated genomes, transcriptomes and DNA genomic data, as well as raw
417 Illumina reads, which highly improved the taxon sampling in the phylogenetic analysis.

418
419 To test the universality of VEHoP across diverse taxa, we employed catfish and insect datasets
420 for testing, comparing the results with those of Read2Tree and MIKE. In these two benchmark
421 tests, the tree generated based on well-annotated genomes was chosen as the reference topology.
422 VEHoP successfully reproduced the same branch orders as that of the reference topology in
423 both cases. In the catfish datasets, all results generated by VEHoP exhibited a high degree of
424 consistency with 100% support for all nodes. In contrast, Read2Tree and MIKE misclassified
425 outgroup species within the ingroup catfishes. Regarding the insect datasets, VEHoP
426 effectively recovered both Hemiptera and Thysanoptera as monophyletic groups with high

427 bootstrap support value. But in Read2Tree, Thysanoptera was found to be paraphyletic.
428 Moreover, in MIKE, none of the orders were recovered as monophyletic. These findings
429 indicate that assemble-free phylogenomic methods still have certain limitations. The
430 inconsistency was also shown in the root-to-tip distance analysis.

431
432 We applied VEHoP to resolve the evolutionary history of the deep-sea gastropod order
433 Neomphalida, which mostly lacks high-quality genome assemblies (unlike the three
434 benchmarking tests). The topology shown on Fig. 3 obtained by VEHoP is identical to
435 ‘topology 1’ in a former study using mitochondrial genomes (Zhang et al. 2024), which lends
436 further support to the hypothesis of multiple habitat transitions from non-chemosynthetic deep
437 sea to various chemosynthetic habitats, i.e., hot vent, sunken wood, or even inactive vent, over
438 the evolutionary history of Neomphalida (Chen et al. 2024). These results indicate that
439 phylogenomic analyses using VEHoP are more robust than phylogenetic analyses using
440 mitochondrial genomes and the other two published software (i.e., MIKE and Read2Tree).

441
442 We acknowledge that VEHoP currently has several limitations: 1) In some uncommon cases
443 (not shown in this work), HmmCleaner.pl or BMGE appeared to get ‘stuck’ on a single OG,
444 taking up to thousands of minutes on a single OG. 2) The data size imbalance of raw reads may
445 result in unstable topology through VEHoP, such as data from organisms with extremely low
446 read coverage ($< 2X$). This might also lead to the expurgation of some taxa, if the strict
447 occupancy criteria (e.g. $>80\%$) is applied. Therefore, adjustment of occupancy and length
448 thresholds are recommended when processing low-coverage sequenced samples. 3) So far,
449 VEHoP is only compiled for use in the Linux system. We are improving the pipeline to make
450 it more widely accessible (e.g., on Windows system).

451
452 With VEHoP, users can define a highly customizable dataset for reference, and it can be a
453 concatenation of high-quality genomes of related species, not limited by an online orthology
454 database, which might result in much more homologs for ortholog inference. The ortholog
455 inference procedure used in VEHoP has been shown to work well in metazoan (Kocot et al.
456 2019; Sun et al. 2020; Sun et al. 2021) and bacterial (Li et al. 2023) datasets. With VEHoP,
457 every ortholog that passes the filtering steps is kept, and the user can determine which ones to
458 eliminate based on other criteria if desired, after the process has been completed. In the output
459 folder, the orthologs, concatenated matrix, as well as related partition file will be available for
460 further deep-phylogeny analyses if necessary. Overall, VEHoP shows many advantages,
461 including fast, accurate, and user-friendly. Importantly, VEHoP makes it possible to utilize and
462 combine genomic DNA and transcriptome data widely available in SRAs. We foresee that a
463 wide application of VEHoP would alleviate the problem of low taxon sampling in the
464 phylogenetic analysis of many groups of organisms.

465

466 **Author Contributions**

467 JS and YL conceived the project. YL coded the pipeline. CC collected the samples. YL and XL
468 carried out the phylogenetic analyses (i.e., draft genome assembly, benchmarks, reanalysis of
469 public data) and manuscript preparation. All authors contributed to the revision of the
470 manuscript.

471

472 **Acknowledgements**

473 This research was financially supported by the National Key Research and Development
474 Program of China (2024YFC2816100), Science and Technology Innovation Project of Laoshan
475 Laboratory (LSKJ202203104), Natural Science Foundation of Shandong Province
476 (ZR2023JQ014), Fundamental Research Funds for the Central Universities (202172002 and
477 202241002), and the Young Taishan Scholars Program of Shandong Province (tsqn202103036).
478 The *Neomphalus fretterae* specimen used herein was collected during R/V *Falkor (too)* cruise
479 FKt231024 (Project Zombie: Bringing dead vents to life – Ultra fine-scale seafloor mapping”)
480 funded by the Schmidt Ocean Institute. We thank the captain and crew of R/V *Falkor (too)* as
481 well as the ROV *SuBastian* team for their immense support of our science. John W. Jamieson
482 (Memorial University of Newfoundland), the chief scientist of cruise FKt231024, is gratefully
483 acknowledged for his diligent execution of the research cruise.

484

485 **Data Availability**

486 The raw reads from the newly sequenced Neomphalida are deposited in NCBI BioProject
487 (accession number: PRJNA1129887). All the raw inputs (draft genomes, transcripts, and
488 proteins) used, and matrixes generated in this work are available at Figshare
489 (<https://doi.org/10.6084/m9.figshare.26370955.v1> including oyster dataset and
490 <https://doi.org/10.6084/m9.figshare.28189616.v1> for fish and insect datasets.). For further
491 enquiries on how to use the VEHoP pipeline, please feel free to contact the corresponding
492 authors.

493

494 **Code Availability**

495 The package of VEHoP is available at <https://github.com/ylify/VEHoP/>.

496

497 **References**

- 498 Ahmed M, Roberts NG, Adediran F, Smythe AB, Kocot KM, Holovachov O (2022)
499 Phylogenomic Analysis of the Phylum Nematoda: Conflicts and Congruences With
500 Morphology, 18S rRNA, and Mitogenomes. *Frontiers in Ecology and Evolution* 9, 769565.
501 Chang C-W, Lyu P-C, Arita M (2011) Reconstructing phylogeny from metabolic substrate-
502 product relationships. *BMC Bioinformatics* 12:S27.
503 Chen C, Li Y, Sun J, Beaulieu SE, Mullineaux LS (2024) Two new melanodrymiid snails from
504 the East Pacific Rise indicate the potential role of inactive vents as evolutionary stepping-stones.
505 *Systematics and Biodiversity* 22:2294014.
506 Cheng H, Concepcion GT, Feng X, Zhang H, Li H. 2021. Haplotype-resolved de novo
507 assembly using phased assembly graphs with hifiasm. *Nature Methods* 18:170-175.
508 Cheon S, Zhang J, Park C (2020) Is phylotranscriptomics as reliable as phylogenomics?
509 *Molecular Biology and Evolution* 37:3672-3683.
510 Criscuolo A, Gribaldo S (2010) BMGE (Block Mapping and Gathering with Entropy): a new
511 software for selection of phylogenetic informative regions from multiple sequence alignments.
512 *BMC Ecology and Evolution* 10:210.
513 Degnan JH, Rosenberg NA (2006) Discordance of species trees with their most likely gene
514 trees. *PLOS Genetics* 2:e68.
515 Di Franco A, Poujol R, Baurain D, Philippe H (2019) Evaluating the usefulness of alignment
516 filtering methods to reduce the impact of errors on evolutionary inferences. *BMC Evol Biol*
517 19:21.
518 Donath A, Jühling F, Al-Arab M, Bernhart SH, Reinhardt F, Stadler PF, Middendorf M, Bernt
519 M (2019) Improved annotation of protein-coding genes boundaries in metazoan mitochondrial
520 genomes. *Nucleic Acids Research* 47:10543-10552.
521 Doolittle WF (1999) Phylogenetic Classification and the Universal Tree. *Science* 284:2124-
522 2128.
523 Doolittle WF, Logsdon Jr JM (1998) Archaeal genomics: Do archaea have a mixed heritage?
524 *Current Biology* 8:R209-R211.
525 Douglas (2018) TransDecoder/TransDecoder. GitHub. Available from:
526 <https://github.com/TransDecoder/TransDecoder> (accessed March 23, 2020).
527 Dunn CW, Hejnal A, Matus DQ, Pang K, Browne WE, Smith SA, Seaver E, Rouse GW, Obst
528 M, Edgecombe GD, Sørensen MV, Haddock SH, Schmidt-Rhaesa A, Okusu A, Kristensen RM,
529 Wheeler WC, Martindale MQ, Giribet G (2008) Broad phylogenomic sampling improves
530 resolution of the animal tree of life. *Nature* 452:745-749.
531 Dylus D, Altenhoff A, Majidian S, Sedlazeck FJ, Dessimoz C (2024) Inference of phylogenetic
532 trees directly from raw sequencing reads using Read2Tree. *Nature Biotechnology* 42:139–147
533 Emms DM, Kelly S (2019) OrthoFinder: phylogenetic orthology inference for comparative
534 genomics. *Genome Biology* 20:238.
535 Fleming JF, Valero-Gracia A, Struck TH (2023) Identifying and addressing methodological
536 incongruence in phylogenomics: A review. *Evolutionary Applications* 16:1087-1104.
537 Fu L, Niu B, Zhu Z, Wu S, Li W (2012) CD-HIT: accelerated for clustering the next-generation
538 sequencing data. *Bioinformatics* 28:3150-3152.
539 Ghiselli F, Gomes-Dos-Santos A, Adema CM, Lopes-Lima M, Sharbrough J, Boore JL (2021)
540 Molluscan mitochondrial genomes break the rules. *Philosophical Transactions of the Royal
541 Society B* 376:20200159.
542 Hao Y, Kajihara H, Chernyshev AV, Okazaki RK, Sun SC (2015) DNA Taxonomy of
543 Paranemertes (Nemertea: Hoplonemertea) with spirally fluted stylets. *Zoology* 32:571-578.
544 Haas BJ, Papanicolaou A, Yassour M, Grabherr M, Blood PD, Bowden J, Couger MB, Eccles
545 D, Li B, Lieber M, MacManes MD, Ott M, Orvis J, Pochet N, Strozzi F, Weeks N, Westerman
546 R, William T, Dewey CN, Henschel R, LeDuc RD, Friedman N, Regev A (2013) De novo
547 transcript sequence reconstruction from RNA-seq using the Trinity platform for reference
548 generation and analysis. *Nat Protoc* 8:1494-1512. Huynen MA, Bork P (1998) Measuring
549 genome evolution. *Proceedings of the National Academy of Sciences of the United States of
550 America* 95:5849-5856.
551 Ibáñez CM, Eernisse DJ, Méndez MA, Valladares M, Sellanes J, Sirenko BI, Pardo-Gandarillas
552 MC (2019) Phylogeny, divergence times and species delimitation of *Tonicia* (Polyplacophora:
553 Chitonidae) from the eastern Pacific Ocean. *Zoological Journal of the Linnean Society*

- 554 186:915-933.
- 555 Irisarri I, Uribe JE, Eernisse DJ, Zardoya R (2020) A mitogenomic phylogeny of chitons
- 556 (Mollusca: Polyplacophora). *BMC Ecology and Evolution* 20:22.
- 557 Katoh K, Standley DM (2013) MAFFT multiple sequence alignment software version 7:
- 558 improvements in performance and usability. *Molecular Biology and Evolution* 30:772-780.
- 559 Kocot KM, Cannon JT, Todt C, Citarella MR, Kohn AB, Meyer A, Santos SR, Schander C,
- 560 Moroz LL, Lieb B, Halanych KM (2011) Phylogenomics reveals deep molluscan relationships.
- 561 *Nature* 477:452-456.
- 562 Kocot KM, Todt C, Mikkelsen NT, Halanych KM (2019) Phylogenomics of Aplacophora
- 563 (Mollusca, Aculifera) and a solenogaster without a foot. *Proceedings of the Royal Society B:*
- 564 *Biological Sciences* 286:20190115.
- 565 Lartillot N, Rodrigue N, Stubbs D, Richer J (2013) PhyloBayes MPI: Phylogenetic
- 566 reconstruction with infinite mixtures of profiles in a parallel environment. *Systematic Biology*
- 567 62:611-615.
- 568 Lee Michael SY, Palci A (2015) Morphological phylogenetics in the genomic age. *Current*
- 569 *Biology* 25:R922-R929.
- 570 Li C, Kou Q, Zhang Z, Hu L, Huang W, Cui Z, Liu Y, Ma P, Wang H (2021) Reconstruction of
- 571 the evolutionary biogeography reveal the origins and diversification of oysters (Bivalvia:
- 572 Ostreidae). *Mol Phylogen Evol* 164:107268.
- 573 Li D, Liu C-M, Luo R, Sadakane K, Lam T-W (2015) MEGAHIT: an ultra-fast single-node
- 574 solution for large and complex metagenomics assembly via succinct de Bruijn graph.
- 575 *Bioinformatics* 31:1674-1676.
- 576 Li H (2023) Protein-to-genome alignment with miniprot. *Bioinformatics* 39:btad014.
- 577 Li Y, He X, Lin Y, Li YX, Kamenev GM, Li J, Qiu JW, Sun J (2023) Reduced chemosymbiont
- 578 genome in the methane seep thyasirid and the cooperated metabolisms in the holobiont under
- 579 anaerobic sediment. *Molecular Ecology Resources* 23:1853-1867.
- 580 Liu X, Sigwart JD, Sun J (2023) Phylogenomic analyses shed light on the relationships of
- 581 chiton superfamilies and shell-eye evolution. *Marine Life Science & Technology* 5:525-537.
- 582 Lozano-Fernandez J (2022) A practical guide to design and assess a phylogenomic study.
- 583 *Genome Biology and Evolution* 14:evac129.
- 584 Marshall CR (2017) Five palaeobiological laws needed to understand the evolution of the living
- 585 biota. *Nature Ecology & Evolution* 1:0165.
- 586 Minh BQ, Schmidt HA, Chernomor O, Schrempf D, Woodhams MD, von Haeseler A, Lanfear
- 587 R (2020) IQ-TREE 2: New models and efficient methods for phylogenetic inference in the
- 588 genomic era. *Molecular Biology and Evolution* 37:1530-1534.
- 589 Mirarab S, Reaz R, Bayzid MS, Zimmermann T, Swenson MS, Warnow T (2014) ASTRAL:
- 590 genome-scale coalescent-based species tree estimation. *Bioinformatics* 30:i541-i548.
- 591 Mongiardino Koch N (2021) Phylogenomic subsampling and the search for phylogenetically
- 592 reliable loci. *Molecular Biology and Evolution* 38:4025-4038.
- 593 Nei M, Kumar S (2000). *Molecular evolution and phylogenetics*, Oxford University Press,
- 594 USA.
- 595 Powell CLE, Battistuzzi FU (2022). *Testing Phylogenetic Stability with Variable Taxon*
- 596 *Sampling. Environmental Microbial Evolution: Methods and Protocols*. H. Luo. New York, NY,
- 597 Springer US: 167-188.
- 598 Price MN, Dehal PS, Arkin AP (2010) FastTree 2 – Approximately Maximum-Likelihood
- 599 Trees for Large Alignments. *PLoS One* 5:e9490.
- 600 Shafin K, Pesout T, Lorig-Roach R, Haukness M, Olsen HE, Bosworth C, Armstrong J, Tigy
- 601 K, Maurer N, Koren S, et al. 2020. Nanopore sequencing and the Shasta toolkit enable efficient
- 602 de novo assembly of eleven human genomes. *Nature Biotechnology* 38:1044-1053.
- 603 Simão FA, Waterhouse RM, Ioannidis P, Kriventseva EV, Zdobnov EM (2015) BUSCO:
- 604 assessing genome assembly and annotation completeness with single-copy orthologs.
- 605 *Bioinformatics* 31:3210-3212.
- 606 Sun J, Chen C, Miyamoto N, Li R, Sigwart JD, Xu T, Sun Y, Wong WC, Ip JCH, Zhang W,
- 607 Lan Y, Bissessur D, Watsuji TO, Watanabe HK, Takaki Y, Ikeo K, Fujii N, Yoshitake K, Qiu
- 608 JW, Takai K, Qian PY (2020) The Scaly-foot Snail genome and implications for the origins of
- 609 biomineralised armour. *Nature Communications* 11:1657.
- 610 Sun J, Li R, Chen C, Sigwart JD, Kocot KM (2021) Benchmarking Oxford Nanopore read
- 611 assemblers for high-quality molluscan genomes. *Proceedings of the Royal Society B:*

612 Biological Sciences 376:20200160.
613 Turnbull R, Steenwyk J, Mutch S, Scholten P, Salazar V, Birch J, Verbruggen H (2023).
614 OrthoFlow: phylogenomic analysis and diagnostics with one command.
615 <https://doi.org/10.21203/rs.3.rs-3699210/v1>
616 Wang F, Wang Y, Zeng X, Zhang S, Yu J, Li D, Zhang X (2024) MIKE: an ultrafast, assembly-,
617 and alignment-free approach for phylogenetic tree construction. *Bioinformatics* 40:btac154.
618 Xie P, Guo Y, Teng Y, Zhou W, Yu Y (2024) GeneMiner: A tool for extracting phylogenetic
619 markers from next-generation sequencing data. *Molecular Ecology Resources*:e13924.
620 Yang Y, Smith SA (2014) Orthology inference in nonmodel organisms using transcriptomes
621 and low-coverage genomes: improving accuracy and matrix occupancy for phylogenomics.
622 *Molecular Biology and Evolution* 31:3081-3092.
623 Young AD, Gillung JP (2020) Phylogenomics — principles, opportunities and pitfalls of big-
624 data phylogenetics. *Syst Entomol* 45:225-247.
625 Zhang L, Gu X, Chen C, He X, Qi Y, Sun J (2024) Mitogenome-based phylogeny of the
626 gastropod order Neomphalida points to multiple habitat shifts and a Pacific origin. *Frontiers in*
627 *Marine Science* 10:1341869.
628 Zhong Z, Lan Y, Chen C, Zhou Y, Linse K, Li R, Sun J (2022) New mitogenomes in deep-
629 water endemic Cocculinida and Neomphalida shed light on lineage-specific gene orders in
630 major gastropod clades. *Frontiers in Ecology and Evolution* 10:973485.
631

632 **Figure Legends**

633

634 Fig. 1. The workflow of the VEHoP pipeline. a) supported input data; b) homolog extraction;
635 c) ortholog inference; d) phylogenetic analyses.

636

637 Fig. 2. Results of phylogenomic analyses with different datasets, including Ostreida, fish and
638 insects. a) Ostreida dataset topology comparison between different methods and the reference
639 topologies. b) Ostreida dataset root-to-tip distance analysis. c) fish dataset topology
640 comparison between different methods and the reference topologies. d) fish dataset root-to-tip
641 distance analysis. e) insect dataset topology comparison between different methods and the
642 reference topologies. f) insect dataset root-to-tip distance analysis.

643

644 Fig. 3. Results of phylogenomic analysis using VEHoP on short Illumina sequencing data from
645 Neomphalida. Nodes with blue dots indicate maximal support in all analyses using different
646 methods. *Neomphalus fretterae* was newly sequenced in this study.

647

648 Fig. 4. Available phylogenomic resources for major phyla in the major animal clade
649 Lophotrochozoa enumerated in terms of the number of taxa with published genomes (red),
650 RNA-seq datasets (orange), and DNA genomic assemblies (blue). Sizes of the circles are
651 proportional to the number of species in each phylum.

652

653 Supplementary Fig. 1. Ostreida phylogeny by VEHoP of full-size dataset and reduced datasets,
654 including 1G, 2G, 4G, 6G and 8G.

655

656 Supplementary Fig. 2. Ostreida phylogeny by VEHoP of subsampled *Crassostrea*
657 *hongkongensis* data size test.

658

659 Supplementary Fig. 3. Ostreida phylogeny by ReadTree of full-size dataset and reduced
660 datasets, including 1G, 2G, 4G, 6G and 8G.

661

662 Supplementary Fig. 4. Ostreida phylogeny by MIKE of full-size dataset and reduced datasets,
663 including 1G, 2G, 4G, 6G and 8G.

664

665 Supplementary Fig. 5. Tree topologies of Fish and Insect datasets.

666

667 Supplementary Fig. 6. Mitochondrial genome-based phylogeny of Neomphalida.

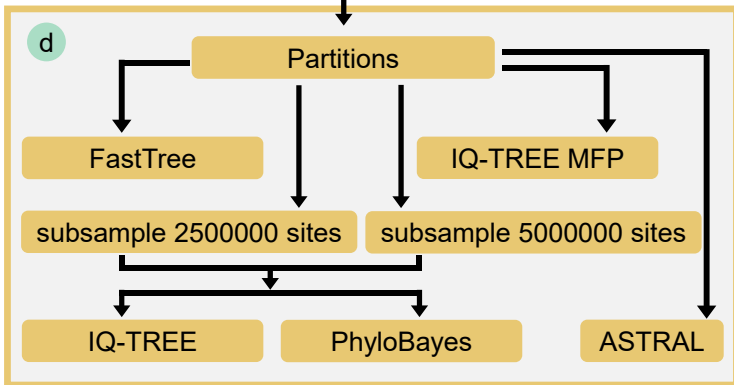
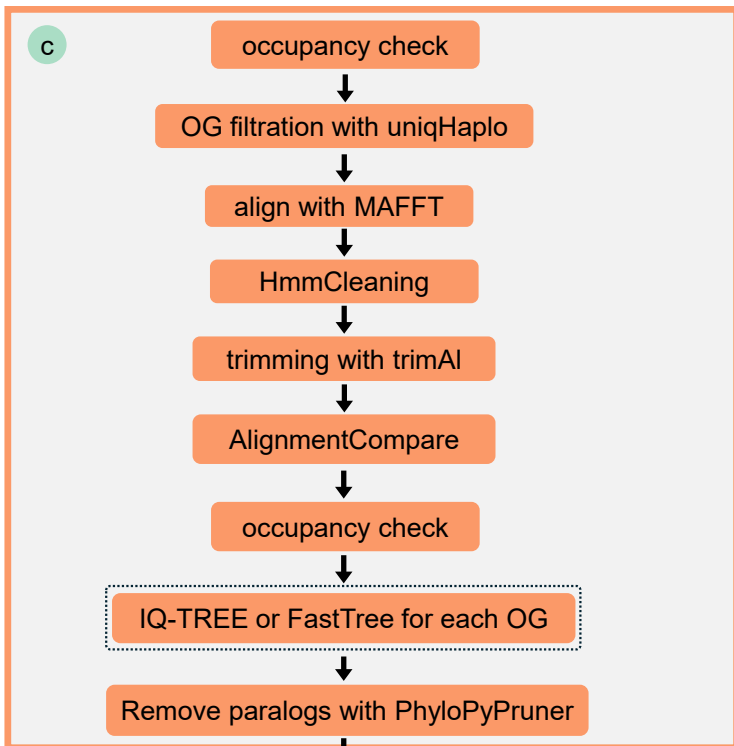
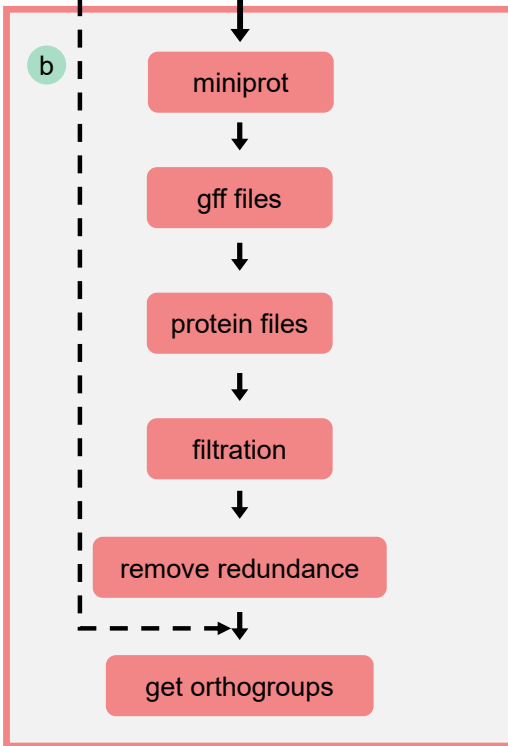
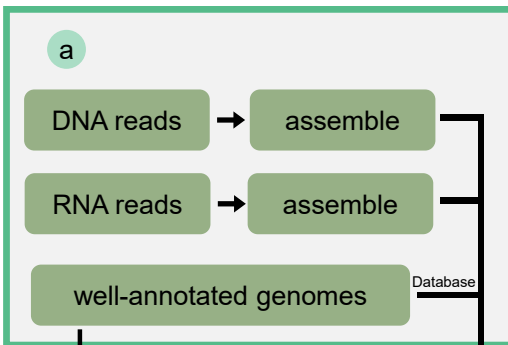
668

669 Supplementary Fig. 7. Neomphalida phylogeny based on NGS data, including VEHoP
670 (multiple models), MIKE and Read2Tree.

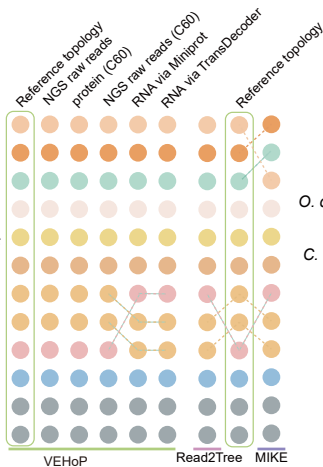
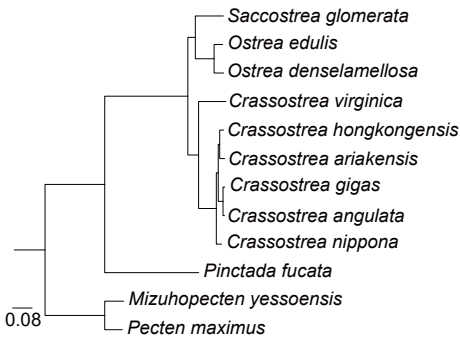
671

672 Supplementary Fig. 8. Occupancy of matrix generated by VEHoP.

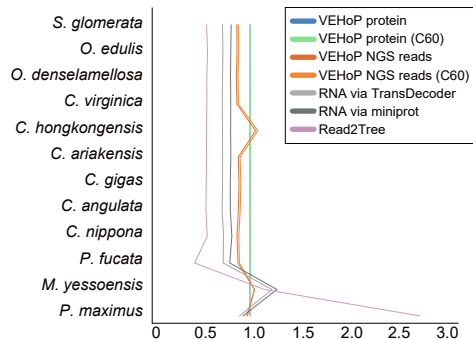
673



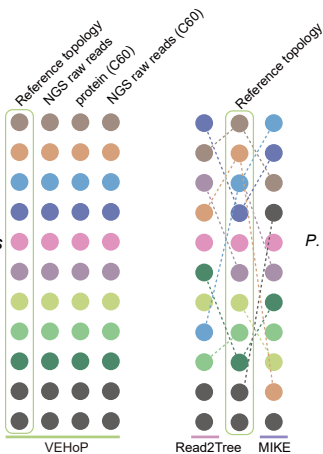
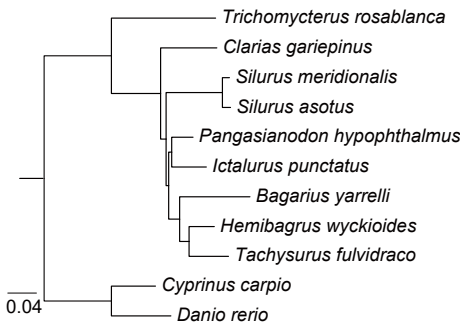
a oysters dataset topologies



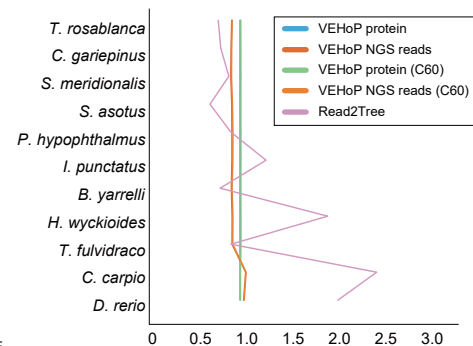
b oysters dataset root-to-tip distance



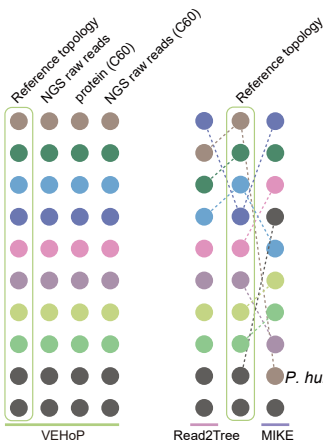
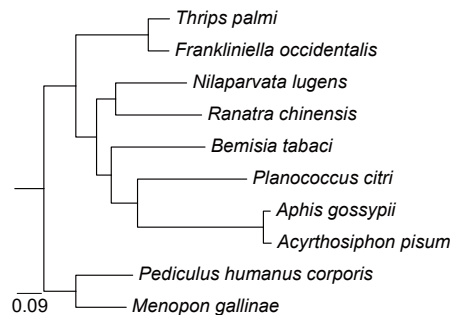
c catfish dataset topologies



d catfish dataset root-to-tip distance



e insects dataset topologies



f insects dataset root-to-tip distance

